Thermoreversible Aggregation and Gelation of Poly(*n*-hexyl Isocyanate)

Jean-Michel Guenet*

Laboratoire d'Ultrasons et de Dynamique des Fluides Complexes, Université Louis Pasteur-CNRS URA 851, 4, rue B. Pascal, F-67070 Strasbourg Cedex, France

Hyun Sik Jeon, Chetan Khatri, Salil K. Jha, Nitash P. Balsara,* and Mark M. Green*

Department of Chemistry and Chemical Engineering and the Herman F. Mark Polymer Research Institute, Polytechnic University, Six Metrotech Center, Brooklyn, New York 11201

Annie Brûlet

Laboratoire Léon Brillouin, CEA-CNRS, CEN Saclay, F-91191 Gif-Sur-Yvette Cedex, France

Annette Thierry

Institut Charles Sadron, Université Louis Pasteur-CNRS, 6, rue Boussingault, F-67083 Strasbourg Cedex, France

Received March 13, 1997; Revised Manuscript Received May 23, 1997[⊗]

ABSTRACT: The molecular and supramolecular structure of poly(*n*-hexyl isocyanate) in *n*-octane has been studied in the sol state and in the gel state by neutron and light scattering. In the sol state the chains appear stiff with dimensional characteristics consistent with the literature on this polymer. The gel consists of a network phase and free chains. The network phase appears to be an array of cross-section polydispersed fibers which can be described with a cross-section radius distribution function of the type $w(r) \sim r^{-1}$ with two cut-off radii $r_{max} = 6.7 \pm 0.4$ nm and $r_{min} = 1.3 \pm 0.1$ nm. These results are compared to the morphology revealed by electron microscopy. The sol state was also studied by dynamic light scattering as a function of concentration, time, and temperature. This revealed the presence of slow and fast modes which could be correlated respectively with the aggregates leading to gelation and to the individual polymer chains. The sol optical activity properties of the pregels revealed a reduction in the population of kinked helical reversals along the backbone consistent with the close parallel packing in the fibers as suggested both by electron microscopy and neutron scattering.

Introduction

Most of the synthetic polymers and biopolymers of various origins can form thermoreversible gels of similar morphologies, i.e. a network constituted of an assembly of fibers[1] with mesh sizes ranging typically from 0.1 to 1 μm. It is thought that thermoreversible gels of this class are formed because of the existence of stiff chains prior to the aggregation process.[2] Chain stiffness can be achieved in several ways for the usually flexible polymers but is an intrinsic property for others such as poly(L-benzyl glutamate) which is known to produce gels in a large variety of solvents.[3]

Since chain-folding is naturally hampered for stiff polymers, the mutual organization of chains cannot give chain-folded crystals whatsoever, and therefore no spherulites, but will produce microfibers instead. This eventually promotes the formation of a gel morphology.

Poly (*n*-hexyl isocyanate), PHIC, also belongs to the category of stiff polymers.[4] The gelation occurring for solutions of this polymer in hydrocarbons has received some attention these past few years, in particular how the chains undergo conformational change before and during aggregation/gelation.[5−7] These conformational changes cause transitions in the optical activity of certain chiral polyisocyanates, a spectroscopic phenomenon connected to the earliest studies of thermally reversible gelation, to gelatin in water,[8] and, more recently, to aggregation events in other polymer systems.[9]

To increase our understanding of the aggregation/gelation phenomenon of this class of polymers we here report on a study of the molecular structure in the sol and the gel states of PHIC in *n*-octane. This system was chosen for its typical behavior in a hydrocarbon solvent, and for the convenience of its gelation temperature. The work reveals the conditions for the aggregation prerequisite to gelation as well as the structure of the fibrous network responsible for the formation of the gel. Time-resolved, dynamic light scattering was used to study the kinetics of aggregation after quenching the system from the sol state (high temperature) to the gel state (low temperature). These experiments were limited to the early stages of gelation in which the solutions were optically clear. With time, the light scattering intensity increased, and eventually an opaque gel was formed. The molecular structure and the morphology of the gelled state were therefore determined by neutron scattering and electron microscopy.

Experimental Section

Materials. PHIC was synthesized following the original Dupont procedure,[10] and the viscosity average molecular weight was determined to be near to 283 000. This was confirmed by gel permeation chromatography[11] which also yielded its polydispersity ($M_w/M_n = 1.79$).

Dynamic Light Scattering (DLS). Solutions for dynamic light scattering were made by encasing predetermined amounts of PHIC (purified by precipitation from a solution which was filtered through a 0.45 μm filter) and anhydrous (filtered through a 0.45 μm filter) *n*-octane in glass cuvettes. These contents of the cuvettes were frozen and evaporated under

[⊗] Abstract published in *Advance ACS Abstracts,* July 15, 1997.

S0024-9297(97)00347-1 CCC: $14.00

vacuum/nitrogen three times and then heat sealed. Three samples with polymer concentrations of C_{pol} = 5, 2.5, and 1 mg/mL were examined. The encased solutions were annealed at 70 °C for 1 h to erase their history and quenched to the experimental temperature as quickly as possible. The dynamic light scattering was monitored as a function of time for several days. The experiments were performed at 20, 25, and 30 °C, and the temperature was controlled to within ±0.1 °C.

Dynamic light scattering data from these solutions of PHIC were obtained on an ALV-5000 instrument, equipped with an argon ion laser (λ = 488.0 nm) as the source for incident light. Data were obtained at several scattering angles between θ = 30° and θ = 150°. Data are reported as a function of the transfer momentum, $q = (4\pi n/\lambda_o)\sin(\theta/2)$, where n is the refractive index of the solution and λ_o is the wavelength of the incident beam in vacuum. The time autocorrelation function of the scattered light intensity, $g(\tau)$, was accumulated in the homodyne mode, and used to obtain the intensity weighted distribution of mobilities, $G(\Gamma)$, by the following equation:[12]

$$g(\tau) = B[a(\int_0^\infty G(\Gamma)\exp(-\Gamma\tau)\,d\Gamma)^2 + 1] \quad (1)$$

Solving eq 1 was achieved by using CONTIN, a software package developed by S. Provencher.[13]

It is also of interest to define the relative area ζ of a peak in a $G(\Gamma)$ vs Γ plot:

$$\zeta = \frac{\int_{\Gamma_1}^{\Gamma_2} G(\Gamma)\,d\Gamma}{\int_o^\infty G(\Gamma)\,d\Gamma} \quad (2)$$

Neutron Scattering. For the neutron scattering experiments, a C_{pol} = 15 mg/mL solution of PHIC in deuterated *n*-octane was prepared directly in a sealed quartz cell by heating at 80 °C and was studied at 70 °C. Gels were obtained by cooling to −18 °C for 24 h. The experiments were performed at the ORPHEE reactor located at the Laboratoire Léon Brillouin (CEN, Saclay, France) on "PAXE", a small-angle camera equipped with a two-dimensional sensitive counter (further detail available on request at LLB). The transfer momentum $q = 4\pi/\lambda_m[\sin\theta/2]$ (λ_m = neutron wavelength and θ the scattering angle) was in the range

$$10^{-1} \le q(\mathrm{nm}^{-1}) \le 1.5 \text{ (for } \lambda = 0.6 \text{ nm)}$$

with a wavelength distribution characterized by a relative full width at half-maximum $\Delta\lambda/\lambda_m \approx 10\%$. The experiments were carried out at 20 ± 1 and 70 ± 1 °C. As usual the spectra were corrected for transmission and thickness and were normalized to an incoherent spectrum of hydrogenated *cis*-decalin. The signal scattered by the deuterated solvent was removed from the total scattered intensity to correct for solvent coherent scattering. The incoherent, flat scattering of the hydrogenated polymer was calculated by means of a method devised by Fazel et al.[14] and subsequently subtracted. The normalized intensity scattered by the protonated polymer is written

$$I_N(q) = KC_H S_H(q) \quad (3)$$

in which C_H and $S_H(q)$ are the concentration and the scattering function of the hydrogenated polymer chains, respectively, and K is a constant which is written

$$K = \frac{4\pi\delta N_A T_{dec}(a_H - n a_D)^2}{g(\lambda) m_o^2 (1 - T_{dec})} \quad (4)$$

in which N_A is Avogadro's number, m_o is the monomer molecular weight, T_{dec} and δ are the *cis*-decalin sample transmission and thickness, respectively, a_H and a_D are the scattering amplitudes of the polymer species and of the solvent, respectively, and $n = d_D m_{oH}/d_H m_{oD}$ in which d_D and d_H are the densities of the solvent and of the monomer and m_D is the solvent molecular weight. $g(\lambda_m)$ is a corrective term which was determined by means of Cotton's method.[15] The absolute intensity is then written

$$I_A(q) = I_N(q)/K \quad (5)$$

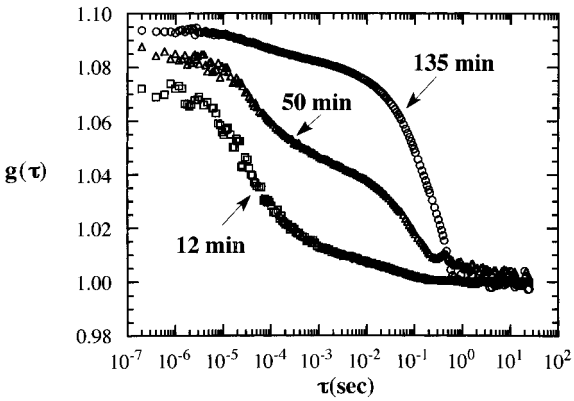

Figure 1. Time autocorrelation function, g(τ), obtained from a PHIC/*n*-octane mixture at 20 °C with C_{pol} = 5 mg/mL, at a scattering angle of θ = 110°. Aging times were as indicated.

Electron Microscopy. Electron microscopy pictures were taken by means of a PHILLIPS CM12 on aggregates obtained from dilute solutions under the same procedure as above. After deposition onto a copper grid of a drop of the solution containing the aggregates, the solvent was evaporated under vacuum, and then the sample was Pt/C shadowed as usual.

Results and Discussion

Dynamic Light Scattering. Typical, time-dependent DLS signals from the 5 mg/mL sample are shown in Figure 1. The autocorrelation functions were obtained at T = 20 °C and at a fixed scattering angle of 110° which corresponds to $q = 29.48\ \mu\mathrm{m}^{-1}$. At the early stage of aggregation (t = 12 min) a rapid decay of the correlation function is seen which indicates high mobility of the diffusing entities in solution. At later times (t = 50 and 135 min) a reduction in mobility is evident. This is quantified in Figure 2 where the distribution of relaxation modes, $G(\Gamma)$, is shown at t = 12 and 135 min. At all times, two relaxation modes are found. With time, the contribution from the fast mode diminishes, and at 135 min, the relaxation spectrum is dominated by the slow mode. The characteristic decay rates, Γ, corresponding to both modes scale linearly with q^2 as expected for a diffusive motion. The diffusion coefficient, $D = \Gamma/q^2$, can be thus estimated and the hydrodynamic radius (R_h) of the diffusion objects can be obtained by using the Stokes−Einstein relationship

$$D = \frac{k_B T}{6\pi\eta_o R_h} \quad (6)$$

where η_o is the solvent viscosity.

The time dependence of R_h corresponding to the fast and slow modes for the 5 mg/mL solution at 20 °C is shown in Figure 3. The corresponding diffusion coefficients are shown on the right-hand *y*-axis in Figure 3. Note that R_h values were computed under the assumption that the solvent viscosity remains constant. The validity of this assumption is discussed later on in this section. This assumption may eventually break down

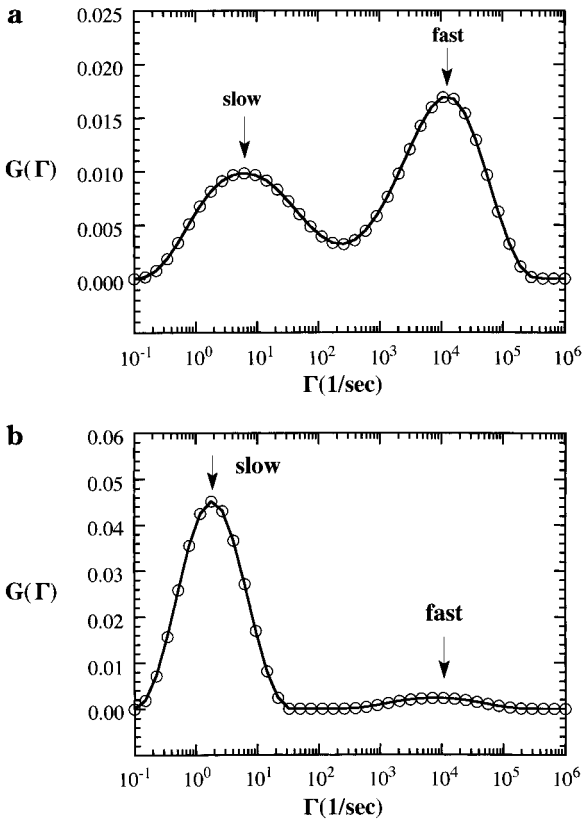

Figure 2. CONTIN results for the distribution of relaxation times, $G(\Gamma)$, obtained a PHIC/*n*-octane mixture with $C_{pol} = 5$ mg/mL, at 20 °C, at a scattering angle of $\theta = 110°$, at a time (a) $t = 12$ min or (b) $t = 135$ min.

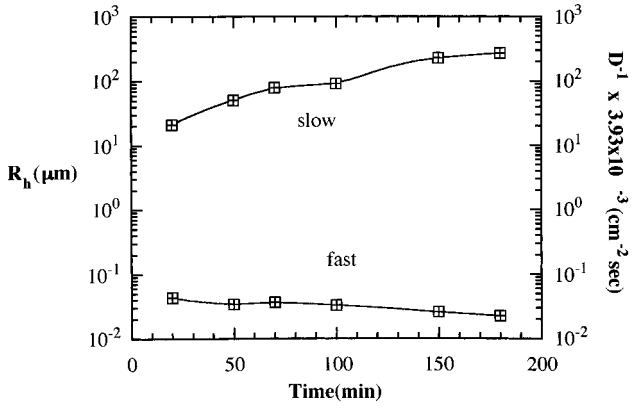

Figure 3. Plot of R_h vs time associated with the fast and slow relaxation modes in a PHIC/*n*-octane mixture with $C_{pol} = 5$ mg/mL, at 20 °C. The corresponding diffusion coefficients are given on the right-hand *y*-axis since R_h and $1/D$ are proportional to each other.

because the system is transforming into a gel, a medium which has an infinite (or nearly so) viscosity.

The R_h value corresponding to the fast mode is consistent with that expected due to Brownian motion of the individual PHIC chains in solution. An estimate of the size of the free chains can be made from the known persistence length of PHIC in *n*-hexane which is assumed to be the same in *n*-octane (40 nm).[11] For a chain with approximately 10 persistence units, which corresponds to the viscosity average molecular weight, one derives $Rg = (10)^{1/2} \times 40/6 = 20$ nm. This is in reasonable agreement with the experimentally determined R_h for the fast mode at 20 °C (30 ± 10 nm). It is worth noting that the presence of the slow mode greatly affects the accuracy with which R_h corresponding to the fast mode can be determined.

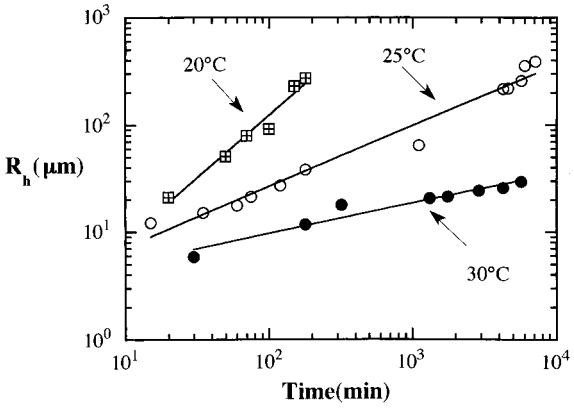

Figure 4. Plot of R_h vs time for PHIC/*n*-octane ($C_{pol} = 5$ mg/mL) solution at different temperatures: circles, 20 °C; triangles, 25 °C; squares, 30 °C.

The slow mode on the other hand, with a characteristic size of $R_h = 10-100$ μm, represents a collection of PHIC chains. At $t = 135$ min, when the sample was removed from the DLS instrument, it appeared clear to the naked eye, and it had the characteristics of a low viscosity (waterlike) fluid. However after several hours at 20 °C, this sample formed a slightly turbid yet still transparent gel. The later stages of gelation were not studied by light scattering due to multiple scattering effects but were studied, as discussed below, by neutron scattering. The aggregates studied by DLS may thus be regarded as precursors to gelation or in other words as *pregels*.

The effect of temperature on the kinetics of aggregation in the $C_{pol} = 5.0$ mg/mL solution is shown in Figure 4. The time dependence of the size of the aggregates, $R_{h,aggregate}$, at temperatures of 20, 25, and 30 °C is plotted. The data can be approximated at all temperatures to power laws with exponents that decrease with inceasing temperature. This indicates that increasing temperature leads to a decrease in the kinetics of aggregation, which is consistent with some organization process.

The DLS data from the $C_{pol} = 2.5$ mg/mL solution was qualitatively similar to those reported above for the $C_{pol} = 5.0$ mg/mL solution. Two modes were observed. In Figure 5a is compared the time dependence of $R_{h,aggregate}$ obtained from the two solutions at 20 °C. The aggregate size and growth rate are seen to diminish with decreasing concentration. The aggregate growth in the $C_{pol} = 2.5$ mg/mL solution is not consistent with a single power law. The aggregation occurs in two stages: a slow early stage followed by a fast late stage. It is possible that the time scale for the early stage in the $C_{pol} = 5.0$ mg/mL was too short to be detected. In Figure 5b is compared the time dependence of ζ from the two solutions. In the times >100 min, $\zeta \approx 1$ for the 5 mg/mL sample, implying that the scattered signal is dominated by the aggregates. This does not necessarily entail that all the free chains have been consumed. It simply means that our technique is insensitive to their presence due to the overwhelmingly large scattering power of the aggregates. These data also support decreased aggregation rates with decreasing concentration.

No aggregation was observed in the solution with $C_{pol} = 1.0$ mg/mL for temperatures 20, 25, and 30 °C. The signal from this solution was too weak to be resolved by the DLS instrument. However, when the sample was

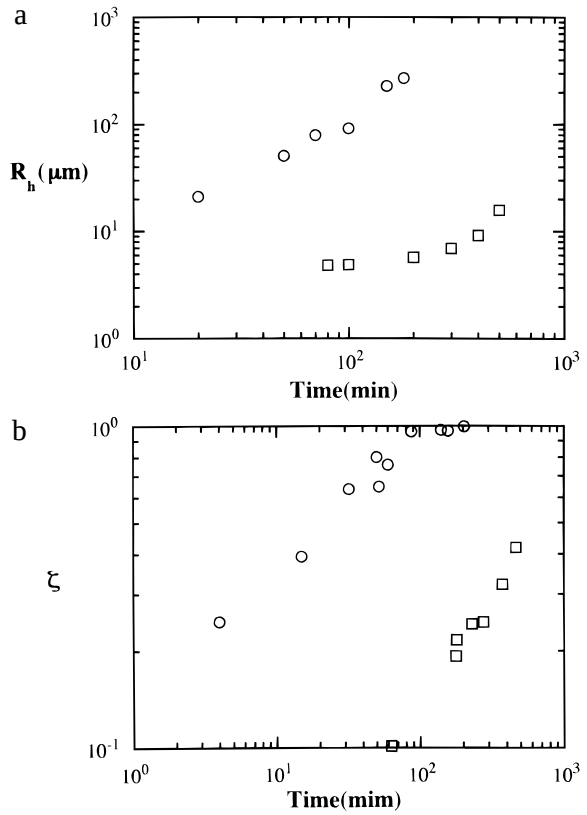

Figure 5. (a) Plot of R_h vs time for PHIC/*n*-octane solutions at different concentrations at 20 °C: circles, 5 mg/mL; squares, 2.5 mg/mL. (b) Plot of ζ vs time for PHIC/*n*-octane solutions at different concentrations at a scattering angle of $\theta = 90°$ and at 20 °C: circles, 5 mg/mL; squares, 2.5 mg/mL.

cooled to 15 °C, an increase in the scattering intensity was observed, and reasonable DLS signals were obtained after a few hours. In Figure 6a is shown $g(\tau)$ at 4.8 and 28.0 h and in Figure 6b the corresponding distribution of mobilities. This aggregation is consistent with the spectroscopic results on dilute solutions which show shifts in the UV bands and strong changes in the optical activity at this temperature.[4,5]

The measurements of the fast relaxation mode obtained from the $C_{pol} = 2.5$ and 5.0 mg/mL solutions at temperatures between 20 and 30 °C do not show any significant dependence on time nor concentration, as expected,since this mode is related to the diffusion coefficient of the free chains. All the measurements of R_h(fast) are scattered around an average value of 35 nm. These data also indicate that the viscosity of the medium surrounding the polymer chains and aggregates does not change appreciably during the pregel forming stage that was studied by light scattering. This indicates that the pregels possessed a mesh size larger than the size of the individual PHIC chains or that their concentration was low.

Neutron Scattering. The sample was studied at 70 °C (solution of individual chains) and 20 °C (gel state). A typical scattering pattern obtained at 70 °C is drawn in Figure 7 by means of a Kratky representation ($q^2I(q)$ vs q). In the low-q range a rodlike behavior is seen ($I_A(q) \sim q^{-1}$) while in the high-q range there appears a significant departure from this behavior. At the lowest q-values no departure from the q^{-1} behavior is apparent, which suggests a large persistence length l_p. Using $l_p = 1.7/q_{min}$,[16] where q_{min} is the smallest value used in these experiments, a lower limiting value of about ≈17 nm is deduced, which indicates a very stiff chain as expected from previous findings.[4]

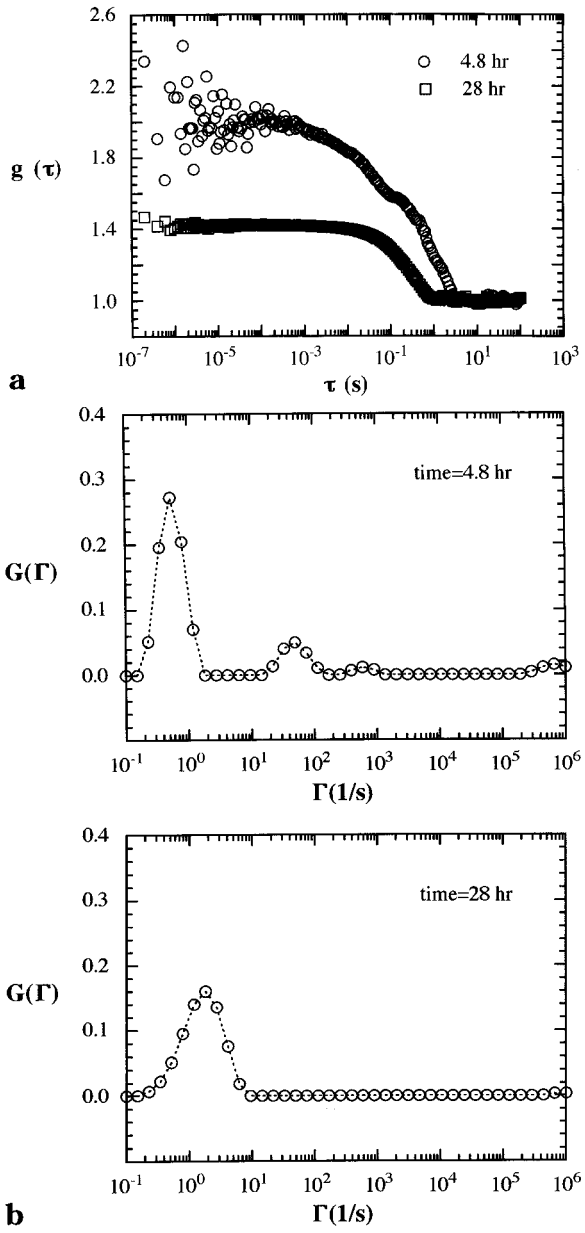

Figure 6. (a) Autocorrelation function g(τ) and (b) the corresponding distribution of mobilities $G(\Gamma)$ for 1mg/mL suspensions at 4.8 and 28 h at $\theta = 90$ °C.

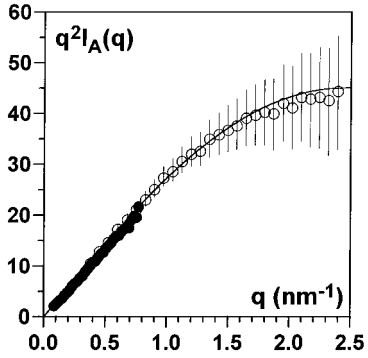

Figure 7. Kratky-plot ($q^2I_A(q)$ vs q) for the sol state ($T = 70$ °C). The solid line represents the best fit (for values see text).

The curve of figure 7 can be fitted with the following equation derived for helices at low resolution which is

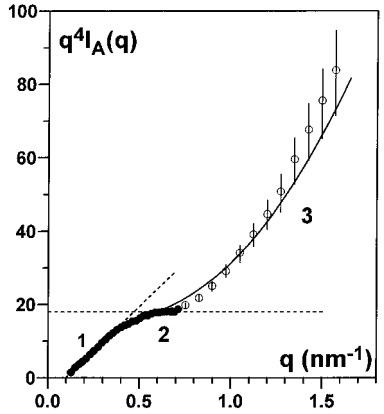

Figure 8. $q^4I_A(q)$ vs q representation for the intensity scattered by a gel obtained after a quench at −18 °C and subsequent annealing at this temperature (24 h). Numbers indicate the different domains: 1 = *transitional*, 2 = *Porod*, and 3 = *asymptotic*.

equivalent to the scattering by solid cylinders[17]

$$I_A(q) \sim \mu_L \frac{4\pi J_1^2(qr_H)}{q^3 r_H^2} \tag{7}$$

in which r_H is the cylinder's cross-section and μ_L the mass per unit length.

From this equation the following values are calculated:

$$\mu_L = 581 \pm 50 \text{ g/(nm mol)}; \; r_H = 0.55 \pm 0.15 \text{ nm}$$

The mass per unit length is close to a value where the chains take on a 8_3 helical form (pitch 0.517 nm, μ_L = 655 g/(nm mol)[18]). The cross-section radius would be consistent with almost-extended hexyl groups, although the low accuracy on the determination of this parameter does not allow one to be definite on this point. The sol state is therefore composed of individual PHIC chains taking on a *loose* helical conformation close to the 8_3 helix.

The same solution, once it was turned into a gel after subsequent annealing at −18 °C, gives the scattering pattern plotted in Figure 8 by means of a $q^4I_A(q)$ vs q representation. Three domains can be distinguished: in domain 1 a linear variation is observed, in domain 2 a plateau is reached, and in domain 3 a significant increase is observed. This scattering pattern can be interpreted by using a model recently derived by Guenet for a network composed of cross-section polydispersed fibers.[19] That the gel is most probably composed of cross-section polydispersed fibers is supported by electron microscopy findings (Figure 9). If the cross-section distribution function is given by

$$w(r) \sim r^{-1} \tag{8}$$

with two cut-off radii r_{min} and r_{max}, then in domain 1 (designated by Guenet[19] as the *transitional q-range*) the intensity is written, provided $ql_n > 1$ (l_n = average network mesh size) as

$$\frac{q^4 I_A(q)}{C_p} = 2\pi^2\rho\left[q - \frac{2}{\pi r_{max}}\right] \times \log^{-1}\left[\frac{r_{max}}{r_{min}}\right] \tag{9}$$

A linear behavior is expected in this range whose

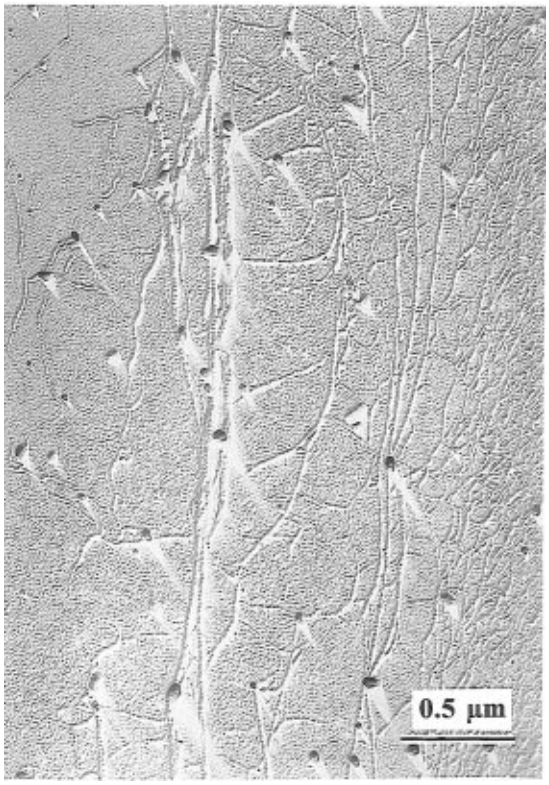

Figure 9. Electron micrographs of microgels prepared from 1.5mg/mL solutions (scale as indicated).

intercept with the q-axis q_o yields r_{max} through

$$r_{max} = \frac{2}{\pi q_o} \tag{10}$$

In domain 2 one observes the Porod regime where the intensity is written[20]

$$\frac{q^4 I_A(q)}{C_p} \simeq \frac{4\pi\rho}{r_n} \tag{11}$$

in which r_n is the number-averaged cross-section radius and reads presently

$$\frac{1}{r_n} = \left[\frac{1}{r_{min}} - \frac{1}{r_{max}}\right] \times \log^{-1}\left(\frac{r_{max}}{r_{min}}\right) \tag{12}$$

Defining q* as the intersect of the straight line of the *transitional regime* with the *Porod plateau* gives r_{min} through the following equation:

$$r_{min} = \frac{2}{\pi q^*} \tag{13}$$

From eqs 10−13 one derives

$$r_{max} = 6.7 \pm 0.4 \text{ nm}; \; r_{min} = 1.3 \pm 0.1 \text{ nm};$$
$$r_n = 1.8 \pm 0.1 \text{ nm}$$

The determinations of both r_{max} and r_{min} are independent of calibration and thus are not affected by any front factor.

Although an accurate determination of these cross-section radii is not possible from the electron micrographs, it can be seen that values derived from the neutron data are consistent with electron microscopy findings. The value of r_{min} suggests that the thinnest

fibers are composed of about seven chains in cross section (this estimate holds provided that the chains possess the same cross-section radius as in the sol state).

Tohyama and Miller have reported on similar observations by electron microscopy on poly [L-benzyl glutamate] (PLBG) thermoreversible gels.[21] It would be of interest to find out whether the same type of cross-section radius distribution as revealed here occurs in this system and more generally in other polypeptides gels.

If the network were only composed of an array of solid fibers the Porod range should extend over all the high q-range. The departure from the plateau regime can be accounted for in two different ways: either due to (i) the *short-range structure of the fibers* or due to (ii) *the presence of free and/or pendant chains.*

(i) If the fiber is no longer compact at short distances (due to solvent intercalation for instance), then the scattering will reflect the spacing apart of the chains through a departure from the Porod regime. This case has been considered for PVC gels.[22] Presently, however, the scattering vector at which the change of behavior occurs suggests a gap of about 3 nm between neighboring chains in the fibers ($q^* \approx 0.7$ nm^{-1}, a rough estimate for this gap can be estimated from $\sim 2/q^*$), which seems rather unrealistic.

(ii) The gel is a two-phase system, where the polymer-rich phase is the network and the polymer-poor phase the pervading liquid. As has been highlighted in the DLS study, this liquid is liable to contain chains that have not been incorporated into the network. The submicronic mesh size of the gel allows these chains to take on a conformation close to that in the sol state. Also, pendant chains, that is chains partially attached to the fibers, may constitute a large part of the gel phase. In both cases, these chains will scatter as individual chains in this q-range. As a result, if $(1 - X)$ is the proportion of free and/or pendant chains, then the intensity should be written

$$q^4 I_A(q) = X q^4 I_{net}(q) + (1 - X) q^4 I_c(q) \qquad (14)$$

in which $I_{net}(q)$ and $I_c(q)$ are the intensities scattered by the network, on the one hand, and by the free and/or pendant chains, on the other hand.

In the *transitional range* as well as at the onset of the *Porod range* $I_{net}(q)$ is far larger than $I_{fc}(q)$ so that the scattered intensity arises mainly from the network but reduced by a factor X. This factor can be ignored as far as the determination of the various values of cross-section radii are concerned. It has to be taken into account, however, for determining the molecular density ρ in the gel phase. At larger q the intensity scattered by the free chains becomes gradually larger than the intensity scattered by the network. The solid line in Figure 8 highlights this effect. This line is calculated by taking the different experimental values determined above, namely $r_n = 1.8$ nm, and $r_H = 0.55$ nm and by taking $X = 0.25$.

The molecular density calculated from eq 14 eventually amounts to $\rho = 687$ g/(nm^3 mol). The actual density can be roughly estimated by assuming in the fibers a close hexagonal packing of the chains while retaining a cross-sectional radius and a mass per unit length close to those measured in the sol state. This estimate yields a theoretical molecular density $\rho_{th} = 554$ g/(nm^3 mol). With regard to the experimental uncertainties on the different parameters, the agreement appears rather satisfying.

The neutron scattering results together with their interpretation therefore suggest the existence of a large amount of free and/or pendant chains in the gel at this concentration. It is worth noting that on aging these gels show noticeable sineresis. Whether there is any link between these two items is a question which remains to be answered.

Concluding Remarks

The complementary experimental approaches taken here enable us to present a picture of the events leading to gelation in PHIC/*n*-octane solutions. In the range of concentrations studied (1−5 mg/mL), heating the sample to 70 °C led to the disintegration of the gel state, and a solution of individual PHIC chains was obtained. When these samples were cooled to temperatures between +35 and −18 °C, we found evidence for slow aggregation of the PHIC chains. At higher concentrations, these aggregates grew in size, and ultimately led to gelation. Although the experiments are unable to detect the initial stages of formation of the pregels, they do show clearly that they grow slowly at the later stages.

In the more concentrated solutions (2.5 and 5 mg/mL), aggregation was found at all temperatures studied while the more dilute solution (1 mg/mL) showed aggregation when quenched to 15 °C. Dynamic light scattering experiments provided direct evidence for the coexistence of free PHIC chains with the aggregates. The relaxation time associated with the aggregates was in the vicinity of 1 s, which is unusually long for these low viscosity materials. This implies that the characteristic size of the aggregates is larger than 1 μm, a figure confirmed by electron microscopy studies.

The structure of the gel state was revealed by neutron scattering. The interpretation of these experiments with a fibrous model where fibers possess cross-section radii ranging from 1.3 to 6.7 nm is consistent with the electron microscopy findings. This means that the cross section of the thinnest fibers is composed of about 7 PHIC chains. The neutron scattering results also suggest that some free chains persist, even in the gel state. In this respect the gel state is similar to the pregel state. Also, here is shown again a case where a sol of semistiff chains produce fibrous gel structures.

The pregel state showed characteristic spectroscopic (UV) and optical activity signatures.[5] In particular, the optical activity results demonstrated a reduction in the number of kinked helix reversals in the chains.[4] This observation indicates the formation of structures composed of parallel, closely packed PHIC chains. The fibrous structures seen in the electron micrographs are consistent with this conclusion. In optical activity experiments, which were carried out on a dilute solution (0.15 mg/mL), the reduction in helix reversal was only seen at 15 °C and not at higher temperatures. This is consistent with the light scattering data presented here for the most dilute solution. This again suggests that pregels are as the gel state, i.e. fibrous structures comprising closely packed PHIC chains.

In spite of a deployment of a variety of experimental tools, that is from dilute solution spectroscopy through scattering experiments to electron microscopy, some questions regarding the thermoreversible gelation of PHIC/*n*-octane solutions could not be answered. For example, the size and shape of the pregels could not be determined. Establishing the mechanism of gel formation requires an insight into the initial stage of the process which our experiments failed to provide.[24] The

role of the solvent in the formation of the fibrous structures (polymer−solvent compound[23]) also remains to be determined.

References and Notes

(1) Guenet, J. M. in *Thermoreversible Gelation of Polymers and Biopolymers*; Academic Press: New York, 1992.
(2) Guenet, J. M. *Trends Polym. Sci.* **1996**, *4*, 6.
(3) For leading references see: Russo, P. S.; Magestro, P.; Miller, W. G. Chapter 11 In *Reversible Polymeric Gels and Related Systems*; Russo, P., Ed.; ACS Symposium Series 350; American Chemical Society: Washington, DC, 1987. Donald, A. M.; Windle, A. H. in *Liquid Crystalline Polymers*; Cambridge University Press: Cambridge, U.K., 1992. Miller, W. G.; Kou, L.; Tohyama, K.; Voltaggio, V. *J. Polym. Sci. Polym. Symp.* **1978**, *65*, 91. Sasaki, N.; Shiwa, S.; Yagihara, S.; Hikishi, K. *Biopolymers* **1983**, *22*, 2539. Tadmor, R.; Cohen, Y. *J. Phys. III* **1993**, *12*, 103.
(4) Green, M. M.; Peterson, N. C.; Sato, T.; Teramoto, A.; Lifson, S. *Science* **1995**, *268*, 1860 and references therein.
(5) Reidy, M. P.; Green, M. M. *Macromolecules* **1990**, *23*, 4225. Yue, S.; Berry, G. C.; Green, M. M. *Polym. Prepr.* **1991**, *32*, 529. Yue, S.; Berry, G. C.; Green, M. M. *Macromolecules* **1996**, *29*, 175. Bouman, M. M.; Meijer, E. W. *Adv. Materials* **1995**, *7*, 385. Green, M. M.; Khatri, C. A.; Reidy, M. P.; Levon, K. *Macromolecules* **1993**, *26*, 4723.
(6) Olayo, H.; Miller, W. G. *J. Polym. Sci., Polym. Phys.* **1991**, *29*, 1473; Turunen, T.; Tenhu, T.; Samarianov, B.; Timofeev, V. P. *Polymer* **1995**, *36*, 4097.
(7) Green, M. M.; Reidy, M. P.; Johnson, R. D.; Darling, D.; O'Leary, D. J.; Willson, G. *J. Am. Chem. Soc.* **1989**, *111*, 6452.
(8) Morawetz, H. *Macromolecules in Solution*, 2nd ed.; Wiley-Interscience Publ.: New York, and references therein.
(9) Reidy, M. P.; Green, M. M. *Macromolecules* **1990**, *23*, 4225. Yue, S.; Berry, G. C.; Green, M. M. *Polym. Prepr.* **1991**, *32*, 529. Yue, S.; Berry, G. C.; Green, M. M. *Macromolecules* **1996**, *29*, 175; Bouman, M. M.; Meijer, E. W. *Adv. Mater.* **1995**, *7*, 385.
(10) Shashoua, V. E.; Sweeney, W.; Tietz, R. F. *J. Am. Chem. Soc.* **1960**, *82*, 866. For recent methods of synthesis of the polyisocyanates, see: Patten, T. E.; Novak, B. M. *J. Am. Chem. Soc* **1996**, *118*, 1906. Okamoto, Y.; Nagamura, Y.; Hatada, K.; Khatri, C.; Green, M. M. *Macromolecules* **1992**, *25*, 5536.
(11) Murakami, H.; Norisuye, T.; Fujita, H. *Macromolecules* **1980**, *13*, 345; Kuwata, M.; Murakami, H.; Norisuye, T.; Fujita, H. *Macromolecules* **1984**, *17*, 2731; Itou, T.; Chikiri, H.; Teramoto, A.; Aharoni, S. M. *Polym. J.* **1988**, *20*, 143.
(12) Berne,B. J.;Pecora,R. *Dynamic Light Scattering*; Wiley: New York, 1976.
(13) Provencher, S. *Makromol. Chem.* **1979**, *180*, 201
(14) Fazel, N.; Brûlet, A.; Guenet, J. M. *Macromolecules* **1994**, *27*, 3836.
(15) Cotton, J. P. In *Neutron, X-ray and light scattering*; Lindner, P., Zemb, T., Eds.; Elsevier: Amsterdam, 1991.
(16) Des Cloizeaux, J. *Macromolecules* **1973**, *6*, 403.
(17) Schmidt, P. W. *J. Appl. Crystallogr.* **1970**, *3*, 257.
(18) Shmueli, U.; Traub, W.; Rosenheck, K. *J. Polym. Sci. Part A2* **1969**, *7*, 515.
(19) Guenet, J. M. *J. Phys. II* **1994**, *4*, 1077.
(20) Porod, G. *Kolloid Z.* **1951**, *124*, 83.
(21) Tohyama, K. and Miller, W. G. *Nature* **1981**, *289*, 813.
(22) Lopez, D.; Dahamani, M.; Mijangos, C.; Brûlet, A.; Guenet, J. M. *Macromolecules* **1994**, *27*, 7415.
(23) Cohen, Y.; Tadmor, R.; Dagan, A. *Macromol. Symp.* **1997**, *114*, 13.
(24) Balsara, N. P.; Lin, C. C.; Hammouda, B. *Phys. Rev. Lett.* **1995**, *77*, 3847.

MA970347V